Available online at www.sciencedirect.com
SCIENCE DIRECT®
Ultramicroscopy 99 (2004) 227–233
ultramicroscopy
www.elsevier.com/locate/ultramic

Shear force distance control in a scanning near-field optical microscope: in resonance excitation of the fiber probe versus out of resonance excitation

D.A. Lapshin[a], V.S. Letokhov[a], G.T. Shubeita[b,1], S.K. Sekatskii[b,*], G. Dietler[b]

[a] *Institute of Spectroscopy Russian Academy of Sciences, Troitsk, Moscow region, 142190, Russia*
[b] *Laboratoire de Physique de la Matière Vivante, IPMC, BSP, Ecole Polytechnique Fédérale de Lausanne, CH-1015 Lausanne-Dorigny, Switzerland*

Received 3 February 2003; received in revised form 20 December 2003; accepted 26 January 2004

Abstract

The experimental results of the direct measurement of the absolute value of interaction force between the fiber probe of a scanning near-field optical microscope (SNOM) operated in shear force mode and a sample, which were performed using combined SNOM-atomic force microscope setup, are discussed for the out-of-resonance fiber probe excitation mode. We demonstrate that the value of the tapping component of the total force for this mode at typical dither amplitudes is of the order of 10 nN and thus is quite comparable with the value of this force for in resonance fiber probe excitation mode. It is also shown that for all modes this force component is essentially smaller than the usually neglected static attraction force, which is of the order of 200 nN. The true contact nature of the tip–sample interaction during the out of resonance mode is proven. From this, we conclude that such a detection mode is very promising for operation in liquids, where other modes encounter great difficulties.

PACS: 07.79.Fc; 46.55.+d

Keywords: Scanning near-field optical microscopy; Shear force

1. Introduction

Scanning near-field optical microscopy (SNOM) is becoming a widely used method in nanotechnology, surface and material physics, biology and other fields (see, e.g. Ref. [1] for a recent review). Nowadays, sharpened optical fibers are the most commonly used sensors in near-field optics, and the shear force method, first proposed in Ref. [2], is usually used to regulate the tip–sample distance. In this technique, the laterally dithered fiber tip interacts with the sample and damping of the oscillation amplitude is used for distance control.

Starting from the pioneering works, dissipative van-der-Waals and capillary forces were discussed as possible explanations for the origin of the shear

*Corresponding author. Tel.: +41-21-693-0445; fax: +41-21-693-0422.
E-mail address: serguei.sekatski@epfl.ch (S.K. Sekatskii).
[1] Present address: Department of Developmental and Cell Biology, School of Biological Sciences, University of California, Irvine, 2302 Natural Sciences I, Irvine, CA 92697-2300, USA.

0304-3991/$ - see front matter © 2004 Elsevier B.V. All rights reserved.
doi:10.1016/j.ultramic.2004.01.003

forces. Later on, Gregor et al. [3]. proposed the so-called non-linear bending force model with a tapping contact caused by a small tilt of the fiber relative to the normal to the surface. This model neglects energy dissipation and considers the transfer of the energy of a vibrating fiber to the sample due to elastic collision. This model and its variations were used to estimate the absolute values of the acting force. For dither amplitudes of 0.1–1 nm (attainable for the tuning fork-based detection) the forces 50–500 pN [4,5] were calculated while for dither amplitudes of the order of 10 nm (optical detection) the value of a few nN [6] was reported. This model seems to be very popular and provides a link between shear force method in scanning optical near-field microscopy and tapping mode in atomic force microscopy (AFM).

However, other authors [7–11] suggest that capillary forces caused by the presence of the thin water adhesion layer on the surface is the main dissipation factor. In Ref. [12] the role of Coulomb forces was emphasized. Lastly, dry contact friction model was put forward for vacuum or low-temperature conditions, hydrophobic surfaces [12] and out of resonance operation [13].

For the better understanding of the origin of the damping, we have measured, using the combined SNOM–AFM setup, the absolute value of force between the probe and a sample [14]. Indeed, our study revealed the importance of Coulomb interaction, as well as the principal role of adhesion water layer for the damping of dither amplitude at ambient conditions. Here, we continue the discussion of the shear force origin and report data not published in Ref. [14]. We mostly concentrate on the out of resonance mode of operation and its comparison with the in resonance mode. It is often taken for granted that use of out of resonance-driven probe is inferior to the resonantly driven one because the interaction force in the former mode should be too large to be used to image fragile (e.g. biological) samples. However, our previous experience of exploiting this operation mode was quite successful: high-quality images of many samples [15], including dried cancer cells [unpublished], were obtained. The results of current experiments, which are presented in this paper, confirm our anticipations: the value of acting force for such an out of resonance detection turns out to be not much larger than the value of the force for the shear force microscopes operated in resonance (included microscopes with tuning fork sensors). This makes the out of resonance mode very attractive due to its obvious applicability in liquids, where using of both optical in resonance- and tuning fork-based shear force detection methods encounters great difficulties [1].

2. Experimental

All experiments were performed in typical indoor winter conditions: temperature of 18–20°C and relative air humidity of 15–25%. The experimental setup combines a home-made SNOM with a home-built AFM, the same as in [14] where further details can be found. The schematic diagram of the setup is shown in Fig. 1 SNOM fiber tip is positioned over the flat

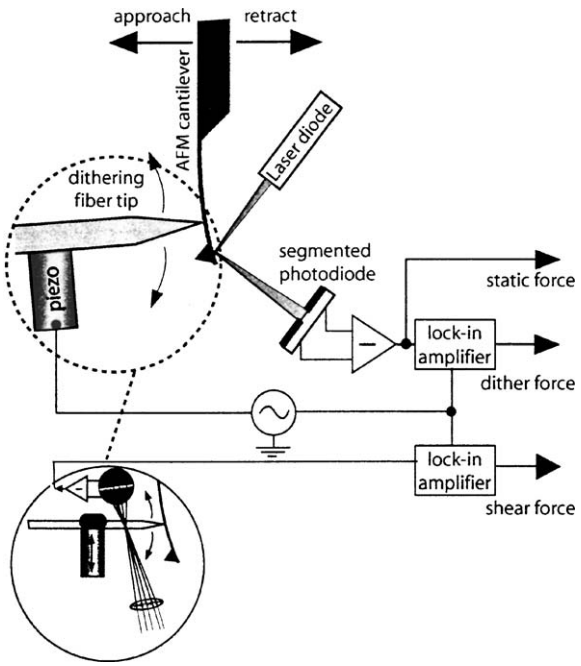

Fig. 1. Schematic diagram of the experimental setup (not to scale). The fiber tip is positioned over the flat portion of the AFM cantilever. The interaction force is measured via the deflection of cantilever. In the inset the optical method of dither amplitude control is shown.

portion of the cantilever. Commercially available Al/Cr-coated straight fiber probes from Nanonics Supertips, Israel, with a nominal aperture of 100–200 nm have been used throughout the study. Absolute values of the forces slightly depend on the concrete probe used (first of all on its radius of curvature, see below), but no principal differences in the behavior of different tips have been observed. Scanning electron microscope inspection of a few tips after the series of measurements did not reveal essential degradation of the tips in a course of experiments.

We utilize only the optical method for controlling dither amplitude in this study. The AFM signal was measured by monitoring the deflection of an external laser-diode light beam from the backside of the cantilever with a second segmented photodiode [16]. Its output voltage U can be easily converted to an absolute force value $F = k\Delta z$ using the known spring constant of the AFM cantilever k and the displacement Δz of the fiber as determined from the voltage applied onto the piezotube. The deflection towards fiber tip is due to the attraction, in opposite direction—to the repulsion. To avoid jumps of cantilever during approach or retraction we used sufficiently stiff cantilevers with nominal spring constants 14 N/m (NSC12/50, NT-MDT, Moscow, Russia) and 40 N/m (RTESP7, Digital Instruments, Santa Barbara, USA). These nominal spring constants were corrected to account for the fact that the force was applied on the cantilever somewhere away from its edge as depicted in Fig. 1.

When the dithered tip approaches to the surface of cantilever, the shear force signal (dither amplitude) and AFM signal (cantilever deflection) are simultaneously recorded. Note, that we found no discernible change in the width or the shape of the shear force approach curve as compared to that when microscope is operated over the solid surface. This gives us reason to believe that there is no significant difference in operation between standard shear force microscope and our experimental setup.

In addition, the dither component of the cantilever deflection was recorded utilizing second lock-in amplifier (see Fig. 1). This force component is due to the tapping of the tip against the surface of cantilever, caused by a small (a few degrees) tilt of the fiber relative to the normal to the surface. This is illustrated by oscilloscope trace of cantilever deflection signal represented in the inset in Fig. 2. The shape of this trace is very different from the sine wave used to excite fiber dithering and shows that the tip is only intermittently touching (tapping) the surface. However, the dither force signal may be observed relatively far from the surface due to electrostatic long-range forces, even when no tapping contact exists [14]. Thus, two components of the force can be distinguished in the cantilever deflection signal. The first is a static averaged deflection caused by a static tip–sample interaction. The second is a dither force component oscillating at the dithering frequency of the tip.

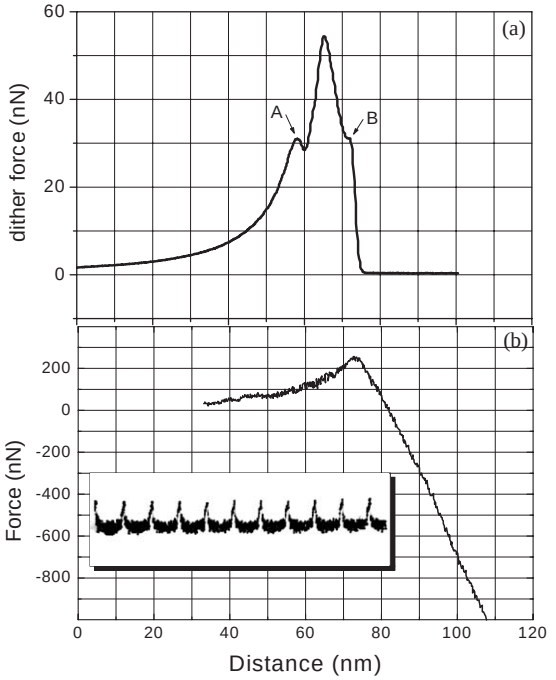

Fig. 2. Approach curves for the dithering force (a) and corresponding cantilever deflection (calibrated in force units), (b) for the resonantly driven probe ($f = 13.8$ kHz, $Q \sim 800$). Dither amplitude—30 nm. In the inset the oscilloscope trace of the AFM cantilever deflection shows peaks due to tapping at the dither frequency of fiber tip.

The dither force signal is a measure of the difference ΔF of the acting force at different

tip–sample distances z and thus it is evidently closely related to the derivative of the force function dF/dz. For a small dither amplitude, the variation of the distance z during the dithering period is $\Delta z = 2\varphi a_{\text{dither}}$ hence, $\Delta F \sim F' a_{\text{dither}}$ Here φ is an angle between the surface normal and the tip; this angle is small (2–4° as measured via an optical microscope) so we do not distinguish between φ and $\sin\varphi$, $\tan\varphi$. If the dither amplitude a_{dither} is constant (far from the surface), the signal of cantilever deflection ΔF is proportional to the derivative of the force function. At small distances this simple relation is corrupted by the drop of a_{dither} caused by tip–surface tapping. Thus, the dither force signal reflects changes in force derivative as well as in amplitude of tip dither.

3. Results and discussion

3.1. Summary for resonance excitation mode

The detailed discussion of the results obtained in resonance mode of operation can be found in Ref. [14]. Here we give a summary of these results. A typical dither force approach curve recorded simultaneously with AFM signal is shown in Fig. 2. The shear force signal is not shown, but the start and the end of shear force associated with points A and B, correspondingly. The point of maximum of AFM graph with subsequent linear slope is associated with repulsion between the tip and the sample. Thus, comparing both graphs, one may conclude that shear force transition is completed upon the contact is established. Analysis of the dependence of the distance $A-B$ on the dithering amplitude of the fiber revealed its nonlinear character at small amplitudes. We interpret this as an evidence of the presence of a 9 nm-thick contaminant (water) layer on the sample surface, as it was often discussed before. These data were presented in our earlier paper [14] and will not be reproduced here.

The maximum dither force (of the order of 10 nN) is observed around the middle point of the transition (see Fig. 2). This can be easily understood: upon approach the tip interacts with the surface for longer periods of time, thus increasing

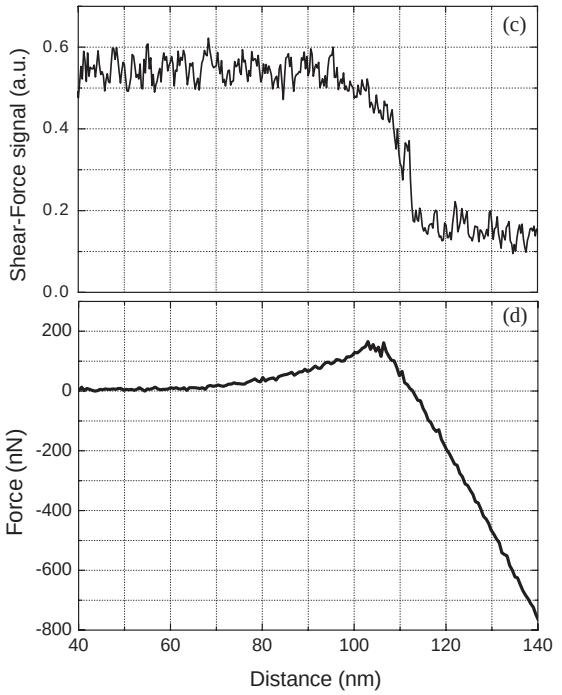

Fig. 3. Approach curves for the shear force signal (c) and corresponding cantilever deflection (calibrated in force units), (d) for the non-resonantly driven probe ($f = 8$ kHz). Dither amplitude—4 nm.

the force exerted. Simultaneously, however, the actual resonance frequency of the probe becomes more and more different from that used for the excitation. This, together with the drop of the Q-factor, leads to the decrease of the dithering amplitude which, in turn, results in decreasing the dither force exerted. The superposition of these two trends gives the function with one maximum in the middle. For a number of applications, operating at the end of shear-force transition looks even more advantageous, because the tip is closer to the real solid surface.

The most important conclusion which can be drawn from these measurements as far as SNOM practice is concerned is the following. The long-range static attractive interaction, which is usually neglected, proved to be very important in our study. The maximal attraction force attains 300 nN (see Fig. 4b) and, thus, essentially exceeds the dither force. Dither force and static force approach curves clearly show that a small

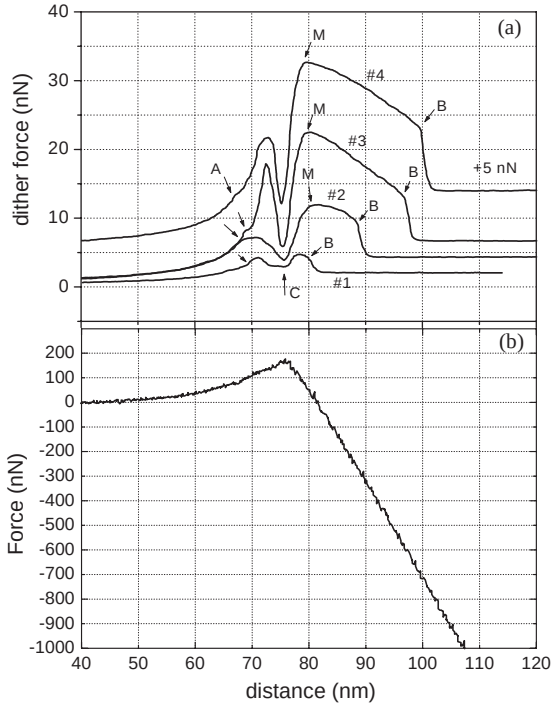

Fig. 4. Approach dither force and static force curves for the non-resonantly driven probe ($f = 8$ kHz), optical detection. Dither amplitude: ♯1—4 nm, ♯2—9 nm, ♯3—14 nm, ♯4—18.5 nm.

attractive force can be detected as far as 100 nm from the surface. At such large distances, as studied in AFM [16,17], the Coulomb force due to localized surface charges and surface potential difference, V, is predominant. By modeling the tip–sample system as a sphere with the radius R located at a distance $z \ll R$ above a flat surface, the Coulomb force is given by [17] $F_c = \pi\varepsilon_0 V^2(R/z)$ The experimental tails of the approach curves can be approximated by functions close to the expected z^{-2} dependence for the derivative of Coulomb force function. Hence, as known from AFM practice, the total force can be essentially decreased by careful regulation of the tip–sample potential difference in the case of conductive samples. This was implemented by us using a cantilever coated with a 10 nm-thick layer of platinum [14]. However, the "bump" of some 300 nN persists on the static AFM approach curve inside the range of shear-force transition. This attractive force probably originates from van der Waals forces and it can be observed with the relatively stiff cantilevers used because of the large radius of the tip being some hundreds of nanometers for the coated fiber probes. This force is usually too small to be routinely seen for normal AFM tips having a small radius of curvature of 10–20 nm.

3.2. Comparison between resonantly and non-resonantly driven probes

Using the same kind of probes and operating in out of resonance excitation mode we recorded shear force, AFM and dither force signals. The results are represented in Figs. 3 and 4. Once again, the maximum of the AFM graph serves as a reference point for contact interaction. Already in Fig. 3 we can see that the end of shear force transition corresponds to the repulsive part of AFM curve. This correspondence becomes much more evident in dither force curves thanks to the low noise signal provided by lock-in technique. The shear force signal remains detectable and continues to decrease even after contact is established. This is what one would expect according to the previously described scenario for a non-resonantly driven tip [13]: the tip goes in permanent contact with the sample while still vibrating.

The dither force approach curve for the case of out of resonance detection (Fig. 4a) may be divided in two parts: (1) from point A (the beginning of shear foirce transition) to point C (point of contact, as indicated by AFM static force curve) and (2) from point C to point B (the end of shear force transition). The first part is obviously associated with tapping behavior, and this was confirmed by oscilloscope traces of AFM deflection analogous to that presented in the inset of Fig. 3. Note that the shape of the curve in this part is similar to dither force approach curves in resonance. The width of this part is 5–9 nm and this is also in accordance with the thickness of adsorption layer (9 nm) deduced from in resonance measurements.

As it is seen from the AFM approach curve, the tip comes in contact with surface after point C, so

the range $C-B$ corresponds to a contact mode with a contact friction as the main dissipation factor for vibrating fiber probe. At the point M corresponding to the maximal force the normal pushing force F_N is minimal and the tip slides along the surface with the largest amplitude. Upon further approach the normal force increases, consequently the friction shear force also increases. As a result, the linear decrease of amplitude is observed until the point B, where the friction force becomes larger than the lateral force supported by the bent fiber. This results in sticking of the tip to the surface and rapid drop of the dither amplitude. One can estimate the friction coefficient μ from the relation $F_N\mu = ka_{dither}$, which should be valid for point B; here k is a fiber's spring constant.[2] Calculated value is 0.6 which is in general agreement with the published values [18,19].

For non-resonantly driven probe, the value of the force in the tapping mode at the beginning of shear force transition is of the same order as for resonantly driven one (about 10 nN). In contact mode (range $C-B$) the static repulsion force is dominant. Note that the total (mostly static) acting force can be even diminished when working in this region, as it is clear from Fig. 4. For example, working close to the point B with dither amplitude of 4 nm (curve #1) one is able to attain the total force value of the order of 30 nN which indeed is *one of the smallest total acting force* registered for all the detection methods studied! (Such a possibility does not exist for other detection modes: shear force transition for resonance mode is over already at the moment of the maximal attractive force, i.e. before the point when the repulsive interaction starts to compensate the attractive one). Definitely, such a circumstance should be considered as an additional advantage of the out of resonance shear force detection. Larger static repulsive forces, typically of the order of 100 nN, can be used with larger dithering amplitude when working in a contact mode.

[2] Neglecting the conical tip, the spring constant for the deflection of the end of the fiber probe in the x and y directions can be calculated as for a rod [16]: $k = 3\pi Er^4/4l^3$ For the length $l \approx 3$ mm, diameter $d = 125$ μm and Youngs modulus E of silica this gives $k \approx 130$ N/m.

Thus for non-resonant excitation, we observed tapping behavior at the beginning of the shear force transition while for resonant excitation only tapping mode is observed. So, evidently, the balance between these modes (tapping–contact) may be changed by tuning the excitation frequency along the shoulder of the resonance curve. Indeed, in Ref. [20] the contact behavior was reported for tuning fork sensor with $Q = 20$.

The contact behavior explains some "strange" observations, in particular, the inversion of contrast in topography (when a "hill" looks like a "pit") on some samples [7,21], as well as exaggerated height near the edge of the step [15]. If we take into account that local friction coefficient may differ from average value, these effects become comprehensible.

Finally, we would like to note that in the literature a few successful attempts to almost completely eliminate the tilt between the probe and the surface by a very careful adjustment of a mutual tip–sample orientation have been reported. Nevertheless, such an adjustment is a very time-consuming and delicate process and by this reason practically it remains a rare option (not to mention that this is possible only for the very flat samples). For such a case it would be hardly feasible to observe the dither signal in the way we did it in this study. However, the main conclusions about the nature of tip–surface interaction remain valid. In particular, we suppose that the adsorption layer will be the principal source of vibration energy dissipation for resonantly excited probe at zero tilt. And contact friction will be the cause for tip amplitude damping for out of resonance excitation.

4. Conclusions

Thus, for shear force-based SNOM, the excitation mode plays crucial role for the nature of interaction as well as for the magnitude of interaction force. Both modes (tapping and contact) may be of use in near-field microscopy. Indeed, the difference between both static and dither force components is not so large for these modes, and in some cases the total acting force for the out of the resonance detection can be even

smaller. As follows from this and others studies, the mechanism of shear force interaction is a very complicated one, which makes the question of the ultimate force sensitivity for different detection schemes really difficult. Further studies, e.g. of the type reported here but performed in UHV conditions, seems are needed to answer it completely.

It also may be argued that the smallest force exerted by the tip on the surface is not always the best mode of operation. In particular, the fluorescence resonance energy transfer probe microscope [22,23] requires that the tip containing a fluorescent molecule is brought close to a counterpart molecule of a sample at a distance smaller than a few nanometers to provide the specific donor–acceptor resonant interaction. The adsorption layers, which are usually present at the surface of the sample at ambient conditions, may hinder such an interaction. To penetrate through such a layer, a contact mode may be an advantage.

We also believe that due to the definitely contact character of the tip–sample interaction for the non-resonantly driven probe, such an option could be used for the quantitative study of the friction phenomenon at different loads, velocities and chemical compositions of (modified) probe and sample. An uttermost importance of such measurements is often highlighted [18,19].

Acknowledgements

This work was supported by the Swiss National Science Foundation Grant No. 2000-065160.01 and SCOPES.

References

[1] M. Ohtsu, Near-Field Nano/Atom Optics and Technology, Springer, Tokyo, 1998;
M.A. Paesler, P.J. Moyer, Near Field Optics Theory: Instrumentation and Applications, Wiley, New York, 1996;
R.C. Dunn, Chem. Rev. 99 (1999) 2891.
[2] E. Betzig, P.L. Finn, J.S. Weiner, Appl. Phys. Lett. 60 (1992) 2484;
R. Toledo-Crow, P.C. Yang, Y. Chen, M. Vaez-Iravani, Appl. Phys. Lett. 60 (1992) 2957.
[3] M.J. Gregor, P.G. Blome, J. Schofer, R.G. Ulbrich, Appl. Phys. Lett. 68 (1996) 307.
[4] K. Karrai, R.D. Grober, Appl. Phys. Lett. 66 (1995) 1842.
[5] J.U. Schmidt, H. Bergander, L.M. Eng, J. Appl. Phys. 87 (2000) 3108;
J.U. Schmidt, H. Bergander, L.M. Eng, Appl. Surf. Sci. 157 (2000) 295.
[6] P.K. Wei, W.S. Fann, J. Appl. Phys. 84 (1998) 4655.
[7] C. Durkan, I.V. Shvets, J. Appl. Phys. 80 (1996) 5659.
[8] S. Davy, M. Spajer, D. Courjon, Appl. Phys. Lett. 73 (1998) 2594.
[9] T. Okajima, S. Hirotsu, Opt. Rev. 5 (1998) 303.
[10] R. Brunner, O. Marti, O. Hollricher, J. Appl. Phys. 86 (1999) 7100.
[11] P.K. Wei, W.S. Fann, J. Appl. Phys. 87 (2000) 2561.
[12] M.-P. Bernal, F. Marquis-Weible, P.-Y. Boillat, P. Lambelet, IEEE Proc. 88 (2000) 1460.
[13] D.A. Lapshin, E.E. Kobylkin, V.S. Letokhov, Ultramicroscopy 83 (2000) 17.
[14] D.A. Lapshin, V.S. Letokhov, G.T. Shubeita, S.K. Sekatskii, G. Dietler, Appl. Phys. Lett. 81 (2002) 1503.
[15] D.A. Lapshin, Tech. Phys. 43 (1998) 1055.
[16] D. Sarid, Scanning Force Microscopy, Oxford University Press, London, 1991.
[17] B. Capella, G. Dietler, Surf. Sci. Rep. 34 (1999) 1.
[18] I.L. Singer, M. Pollock (Eds.), Fundamentals of Friction, Kluwer, Dordrecht, 1992.
[19] B.N.J. Persson, E. Tosatti (Eds.), Physics of Sliding Friction, Kluwer, Dordrecht, 1996.
[20] A.V. Biryukov, S.V. Gaponov, V.L. Mironov, D.G. Volgunov, Phys. Low-Dimens. Str. 3–4 (2001) 17.
[21] H. Heinzelmann, T. Huser, T. Lacoste, H.J. Guntherodt, D.W. Pohl, B. Hecht, L. Novotny, O.J.F. Martin, C.V. Hafner, H. Baggenstos, U.P. Wild, A. Renn, Opt. Eng. 34 (1995) 2441.
[22] R. Dunn, S. Vickery, Biophys. J. 76 (1999) 1812;
R. Dunn, S. Vickery, J. Microsc. 202 (2001) 408.
[23] G.T. Shubeita, S.K. Sekatskii, G. Dietler, V.S. Letokhov, Appl. Phys. Lett. 80 (2002) 2625.